Bioorganic & Medicinal Chemistry Letters 20 (2010) 3103–3106

Contents lists available at ScienceDirect

Bioorganic & Medicinal Chemistry Letters

journal homepage: www.elsevier.com/locate/bmcl

Synthesis of [^{11}C]SSR149415 and preliminary imaging studies using positron emission tomography

Matthias Schönberger [a,b], Carmine Leggett [c], Sung Won Kim [a], Jacob M. Hooker [a,d,e,*]

[a] Brookhaven National Laboratory, Medical Department, Bldg 555, Upton, NY 11973, USA
[b] Johannes Gutenberg University Mainz, Nuclear Chemistry Department, Fritz Strassmann-Weg 2, 55128 Mainz, Germany
[c] University of Louisville School of Medicine, Department of Pharmacology and Toxicology, Louisville, KY 40202, USA
[d] Athinoula A. Martinos Center for Biomedical Imaging, Charlestown, MA 02129, USA
[e] Division of Nuclear Medicine and Molecular Imaging, Massachusetts General Hospital, Harvard Medical School, Boston, MA 02114, USA

ARTICLE INFO

Article history:
Received 8 March 2010
Revised 26 March 2010
Accepted 26 March 2010
Available online 2 April 2010

Keywords:
Positron emission tomography
Vasopressin
SSR149415
Carbon-11

ABSTRACT

SSR149415 was the first non-peptide vasopressin-(V_{1b}) receptor antagonist reported. It has been used to probe the role of V_{1b} receptors in animal models of depression, aggression, and stress-anxiety, and was progressed to clinical trials for the treatment of depression. Due to the interest in V_{1b} receptors as a therapeutic target and the growing use of SSR149415 in preclinical research, we developed a method to label SSR145419 with carbon-11 and have studied its pharmacokinetics in non-human primates using positron emission tomography.

Arginine vasopressin (AVP) is a cyclic disulfide peptide hormone that is synthesized in the hypothalamus, stored in the pituitary, and secreted into the blood.[1] AVP engages several targets including the three unique AVP receptors (V_{1a}, V_{1b}, and V_2) as well as oxytocin receptors. Elevation of AVP in the bloodstream causes antidiuresis and moderate vasoconstriction mediated predominantly by V_{1a} and V_2 receptors and their downstream signaling pathways. V_{1b} receptors (also known as V_3 receptors) are distributed in the central nervous system and modulate release of the stress hormone ACTH in response to AVP.[2] Due to this function, V_{1b} receptors have been implicated as targets for exploring and potentially treating stress-related disorders such as anxiety and depression.[3]

Disclosure of the first non-peptide antagonist of V_{1b}, SSR149415, has facilitated research aimed at improving our understanding of the physiological role that V_{1b} receptors play in stress-related disorders.[4] SSR149415 exhibits low nanomolar inhibition of V_{1b} receptors and 100–1000-fold selectivity over V_{1a}, V_2, and oxytocin receptors. Behavioral pharmacology experiments using SSR149415 have demonstrated its anxiolytic- and antidepressive-like effects as well as its ability to reduce offensive aggression.[5] Furthermore, the use of [^{3}H]SSR149415 for in vitro saturation and autoradiography experiments indicated an interesting binding profile in certain tissues including the pituitary.[6]

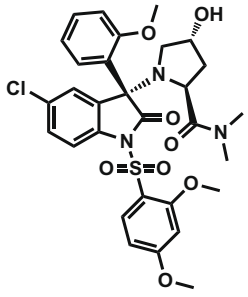

V_{1b} Antagonist
SSR149415

Given the interest in V_{1b} receptor pharmacology and the use of SSR149415 as a therapeutic drug[7] we developed a method to label SSR149415 with carbon-11 to facilitate evaluation of its pharmacokinetics in vivo using positron emission tomography (PET)—a powerful tool for understand drug behavior.[8] Herein, we describe a route for the synthesis of SSR149415, which was adapted from patent literature[9]. This is the first full report of its synthesis, isolation, and characterization data. In addition, we detail our strategy and method to label SSR149415 with carbon-11. Using this strategy we have performed initial in vivo characterization in non-human primates using PET, which indicate that SSR149415 has low blood brain barrier (BBB) penetration and brain uptake.

* Corresponding author.
E-mail address: hooker@nmr.mgh.harvard.edu (J.M. Hooker).

0960-894X/$ - see front matter © 2010 Elsevier Ltd. All rights reserved.
doi:10.1016/j.bmcl.2010.03.108

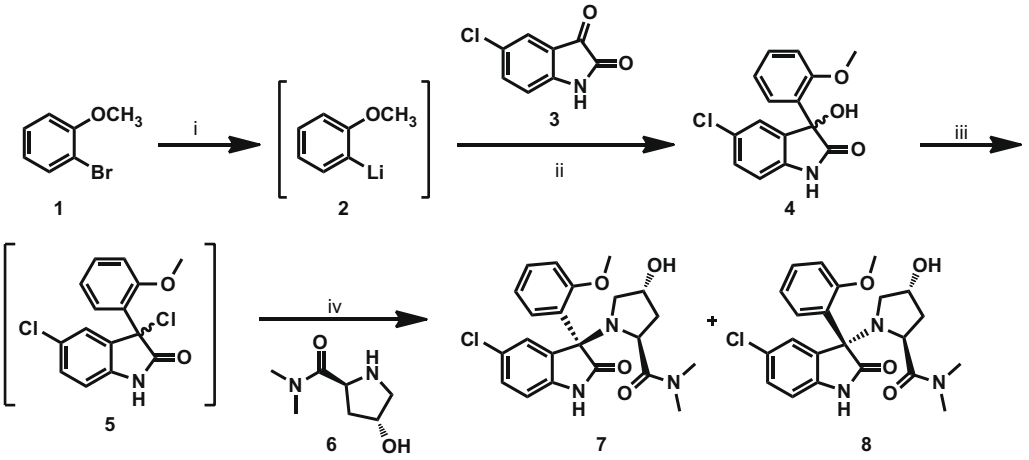

Scheme 1. Synthesis of SSR149415 part 1. Addition of the anisole- and proline derivative to the isatine's carbonyl C-3. Reagents and conditions: (i) *n*BuLi, THF, −78 °C, 10 min; (ii) THF, −78 °C to rt, 30 min, 49%; (iii) $SOCl_2$, Pyr, DCM, 0 °C to rt, 30 min; (iv) TEA, DCM, 0 °C to rt, 48 h, 40% (+/-).

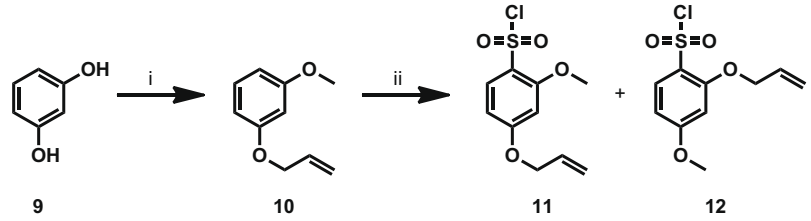

Scheme 2. Functionalization of resorcinol. Reagents and conditions: (i) Allyl bromide, CH_3I, K_2CO_3, acetone, rt to 80 °C, 6 h, 80%; (ii) (1) PCl_5, DCM, 0 °C; (2) SO_3/H_2SO_4, 5 min, 24% (mxt 11/12).

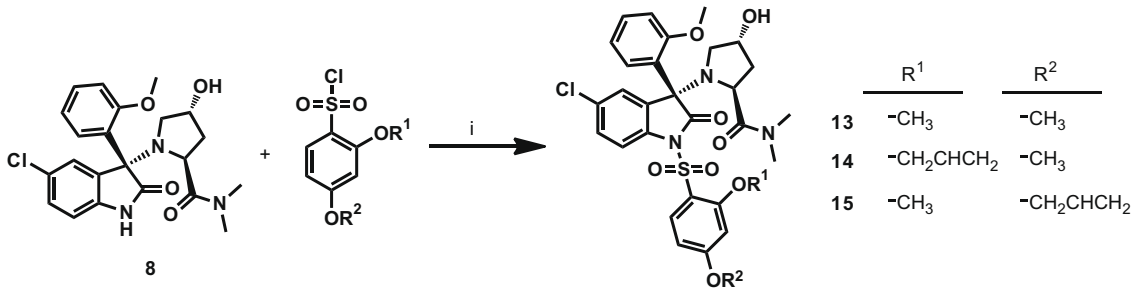

Scheme 3. Synthesis of SSR149415 part 2 and precursor preparation. Reagents and conditions: (i) NaH, DMF, 0 °C, 3 min, quant.

The synthetic procedure for both SSR149415 and a precursor for carbon-11 labeling, was based on additions of pendant groups to a commercially available isatin core, Scheme 1. Although asymmetric additions to isatins are known[10] we chose to perform a racemic synthesis of alcohol **4**, relying on the separation of diastereomers formed in subsequent steps with achiral techniques. To avoid protection of the amide nitrogen in the first step of our scheme, we employed an excess of the aryl lithiate **2** formed from *o*-bromoanisole. The reaction of **2** with **3** occurred quickly at −78 °C and afforded the racemic mixture of **4** in 49% combined yield.

The proline fragment of SS9149415 was derived from commercially available *trans*-4-hydroxy-L-proline in three steps: protection of the proline nitrogen as a benzyl carbamate, formation of the dimethyl amide, and deprotection (see Supplementary data for details). Using this procedure building block **6** was isolated after three steps without chromatography proceeding in 85% overall yield.

To add the proline and isatin fragments, tertiary alcohol **4** was converted to chloride **5** using thionyl chloride. Following removal of the excess thionyl chloride, intermediate **5** was treated with triethylamine and proline fragment **6**. The resulting epimers **7** and **8** were separated by flash chromatography (the identity of the two epimers was later assigned based on optical rotation data following sulfonamide formation and comparison to the Sanofi patent).[9]

To obtain a desmethyl derivative of SSR149415 for use as a carbon-11 precursor, an allyl protected sulfonyl chloride building block was synthesized starting from resorcinol (**9**), Scheme 2. Diether **10** was formed in a one pot from a mixed alkylation reaction using methyl iodide and allyl bromide. Following isolation, compound **10** was treated with excess PCl_5 and fuming sulfuric acid at 0 °C. As expected, both regioisomers **11** and **12** were obtained. Although they could be separated, we found that it was more efficient to carry on the mixture of **11** and **12** and perform the separation during the last step of the precursor synthesis.

Sulfonamide formation at the 'isatin' nitrogen **8** was accomplished with commercially available 2,4-dimethoxybenzene sulfonylchloride and the mixture of **11** and **12**, Scheme 3. Using this

Table 1
Characterization of compounds **7**, **8**, **13** and **16** with chromatography and optical rotation measurements (see Supplementary data)

	7	8	13	16
RT	8.99	7.89	10.18	9.96
R_f	0.50	0.42	0.53	0.51
α_D^{25}	–	–	−0.140	+0.079

Entry 1: Retention times (RT) by HPLC. Entry 2: R_f-values (TLC). Entry 3: Optical rotation, c = 1 mg/mL ($CHCl_3$), b = 1 cm.

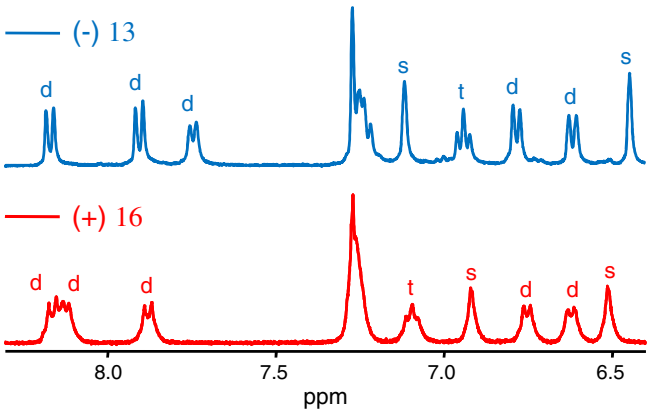

Figure 1. Comparison of SSR149415 (**13**) and its epimer (**16**) of opposite optical rotation using ^{1}H NMR. The aromatic protons can be used for identification.

strategy we obtained SSR149415 (**13**) and two allyl protected precursors for carbon-11 labeling (**14** and **15**). It is worth noting that we also performed these reactions with compound **7** (the epimer of **8**) in order to get full characterization of the epimer of SSR149415 (**16**). The pharmacologically active epimer was previously assigned as the one with a negative optical rotation. Since other labs may want to prepare SSR149415, we have provided Table 1 that summarizes some of the key chromatography and optical rotation information.

Once we had assigned all of the structures based on the patent literature, we found that the most facile technique to identify each epimer was by proton NMR. Figure 1 highlights signals of the aromatic protons showing further separated doublets downfield from the solvent peak and a reversed order of singlet and triplet upfield. This data should help facilitate quick identification of SSR149415 for those preparing it in the future.

Palladium-mediated deallyation of a mixture of **14** and **15** was used to reveal phenol precursors for carbon-11 labeling experiments, Figure 2A (compound **15** is shown singularly for clarity). To accomplish the deprotection the mixture of allyl-aryl ethers

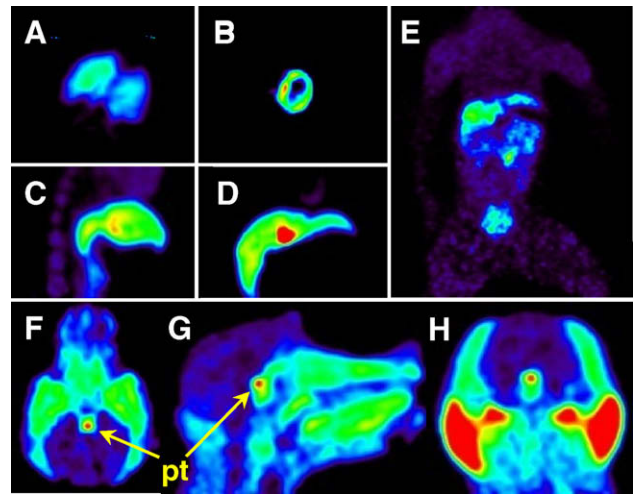

Figure 3. Summed PET images from baboon experiment with [^{11}C]SSR149415. **A**: lung, transverse view, (50–420 s), (B) heart muscle, transverse view, (50–420 s), (C) spine and liver, sagittal view, (50–420 s), (D) liver and gall bladder, coronal view (50–1200 s). (E) Whole body PET scan of a baboon performed after a 90 min dynamic scan. (F) transverse, (G) sagittal and (H) coronal view on brain images centered on pituitary (pt).

14 and **15** was dissolved in DCM and treated with a catalytic amount of $Pd(PPh_3)_4$ followed by dimethylamine. This led to quantitative deprotection after only 10 min at room temperature. The two regioisomers were separated by preparative reversed phase chromatography. With both regioisomers in hand, we investigated methylation (to form SSR149415) and quickly determined that regioisomer **17** was superior in terms of both labeling yields and ease of purification by chromatography.

After a brief period of optimizing the reaction of **17** with [^{11}C]methyl iodide, we found that the highest yielding reactions were realized when the supernatant of a saturated NaOH/DMSO solution was used as solvent/base system at high temperatures (150 °C) and short reaction times (4 min) (see Supplementary data for optimized procedure). Figure 2B provides a representative chromatogram using a radioactivity detector. The radioactive product eluting at the expected SSR149415 retention time was collected, concentrated and analyzed by a variety of chromatography experiments for quality control. We also verified the identity of the peak using LC–MS performing analogous reactions with [^{13}C]methyl iodide.

Following our optimized procedure, we were able to synthesize, isolate, and formulate [^{11}C]SSR149415 in ~40 min from the end of cyclotron bombardment. A typical preparative run produced 3–6 mCi (>2 Ci/μmol) of the final product in injectable saline with 10% EtOH after filtration through a 0.22 μM sterile filter.

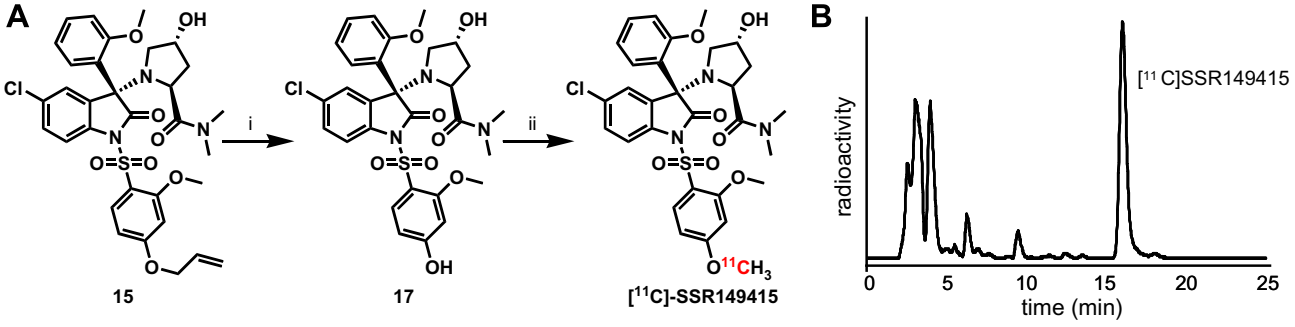

Figure 2. (A) Deallylation revealing precursor and ^{11}C-labeling. (i) $Pd(PPh_3)_4$, DMA, DCM, rt, 10 min, quant.; (ii) [^{11}C]CH_3I, NaOH/DMSO, 150 °C, 4 min. (B) Semipreperative HPLC, radioactive trace (see Supplementary data for LC–MS analysis).

Using [^{11}C]SSR149415 we determined its lipophilicity (log *D*) and propensity for plasma protein binding (PPB). The log *D* value of [^{11}C]SSR149415 received from a series of octanol/water distributions was 3.22 ± 0.67 (n = 16)—well within the accepted log *D* values for passive blood brain barrier penetration of 2.0–3.5.[11] In PPB assays, we determined that only 2.54% ± 0.43% (n = 4) of the compound was in the free fraction of plasma indicating a strong affinity for plasma proteins. The nature or specificity of this interaction was not determined.

Several PET imaging experiments were performed using non-human primates to evaluate the pharmacokinetics and metabolism of [^{11}C]SSR149415. The average dose for the PET imaging experiments using baboons was 2.5 ± 0.8 mCi [^{11}C]SSR149415, which was administered intravenously. Dynamic brain images were collected for 90 min. Following this, the animal position was moved placing the torso in the PET gantry and another injection of [^{11}C]SSR149415 was performed (>2 h after the initial injection). Again a 90 min dynamic acquisition was collected. In addition to these studies, following the final dynamic imaging session, a whole body scan was recorded to determine the gross distribution of radioactivity in the animal at the end of the 90 min acquisition. Starting immediately at the time of injection, blood samples were taken over the course of 60 min and analyzed by HPLC to determine the fraction of carbon-11 which was present as parent compound. Interestingly, after approximately 10 min, the drug was already metabolized to 50%. The entire imaging session was repeated in a second animal.

Summed-images from these experiments are provided in Figure 3 (time-activity curves and metabolism data can be found in the Supplementary data).

Using PET, we determined that SSR149415 and/or its radiolabeled metabolites accumulate predominantly in the liver (0.1–0.25% ID/cc). We observed low yet noticeable accumulation in the heart, spine and lung. These were on the order of 0.01–0.03% ID/cc at their maximum.

Interestingly, we observed very minimal uptake of radioactivity in the non-human primate brain. We surmise that mechanism of action of SSR149415 in behavioral pharmacology experiments is likely not due to interaction of V_{1b} receptors in the brain. However, we did observe a high concentration of radioactivity in the pituitary, which has been reported to possess a high density of V_{1b}-receptors.[12] The saturability of the accumulated radioactivity that we observed has not yet been determined so at this point we cannot comment on whether the binding is specific.

In conclusion, we have developed a method for the synthesis of [^{11}C]SSR149415 and characterized its pharmacokinetic behavior in non-human primates. These data should provide valuable insight into the pharmacological effects that have been observed in behavioral assays using SSR149415.

Acknowledgments

This study was supported by Brookhaven National Laboratory under contract DE-AC02-98CH10886 with the U.S. Department of Energy, supported by its Office of Biological and Environmental Research. Funding for M.S. was provided by the Study Foundation of the German People. The authors are grateful to Dr. Michael Schueller for cyclotron operation and the PET radiochemistry, the imaging team at BNL (Youwen Xu, Colleen Shea, Lisa Muench, David Alexoff, Pauline Carter, Payton King, and Don Warner) for carrying out primate imaging experiments, and to Dr. Joanna Fowler for scientific input and guidance. M.S. acknowledges Prof. Dr. Frank Rösch for advice and support during this work.

Supplementary data

Supplementary data associated with this article can be found, in the online version, at doi:10.1016/j.bmcl.2010.03.108.

References and notes

1. (a) Barberis, C.; Morin, D.; Durroux, T.; Mouillac, B.; Guillon, G.; Seyer, R.; Hibert, M.; Tribollet, E.; Manning, M. *Drug News Perspect.* **1999**, *12*, 279; (b) de Wied, D.; Diamant, M.; Fodor, M. *Front. Neuroendocrinol.* **1993**, *14*, 251.
2. (a) Landgraf, R. *CNS Neurol. Disord. Drug Targets* **2006**, *5*, 167; (b) Ring, R. H. *Curr. Pharm. Des.* **2005**, *11*, 205.
3. (a) Arban, R. *Endocrinology* **2007**, *148*, 4133; (b) Decaux, G.; Soupart, A.; Vassart, G. *Lancet* **2008**, *371*, 1624; (c) Griebel, G.; Simiand, J.; Stemmelin, J.; Gal, C. S.; Steinberg, R. *Curr. Drug Targets CNS Neurol. Disord.* **2003**, *2*, 191; (d) Lemmens-Gruber, R.; Kamyar, M. *Cell Mol. Life Sci.* **2006**, *63*, 1766.
4. (a) Chen, J.; Young, S.; Subburaju, S.; Sheppard, J.; Kiss, A.; Atkinson, H.; Wood, S.; Lightman, S.; Serradeil-Le Gal, C.; Aguilera, G. *Ann. N.Y. Acad. Sci.* **2008**, *1148*, 349; (b) Engin, E.; Treit, D. *Neuropeptides* **2008**, *42*, 411; (c) Griebel, G.; Simiand, J.; Serradeil-Le Gal, C.; Wagnon, J.; Pascal, M.; Scatton, B.; Maffrand, J. P.; Soubrie, P. *Proc. Natl. Acad. Sci. U.S.A.* **2002**, *99*, 6370; (d) Stemmelin, J.; Lukovic, L.; Salome, N.; Griebel, G. *Neuropsychopharmacology* **2005**, *30*, 35.
5. (a) Blanchard, R. J.; Griebel, G.; Farrokhi, C.; Markham, C.; Yang, M.; Blanchard, D. C. *Pharmacol. Biochem. Behav.* **2005**, *80*, 189; (b) Hodgson, R. A.; Higgins, G. A.; Guthrie, D. H.; Lu, S. X.; Pond, A. J.; Mullins, D. E.; Guzzi, M. F.; Parker, E. M.; Varty, G. B. *Pharmacol. Biochem. Behav.* **2007**, *86*, 431; (c) Iijima, M.; Chaki, S. *Prog. Neuropsychopharmacol. Biol. Psychiatry* **2007**, *31*, 622; (d) Overstreet, D. H.; Griebel, G. *Pharmacol. Biochem. Behav.* **2005**, *82*, 223; (e) Serradeil-Le Gal, C.; Wagnon, J.; Simiand, J.; Griebel, G.; Lacour, C.; Guillon, G.; Barberis, C.; Brossard, G.; Soubrie, P.; Nisato, D.; Pascal, M.; Pruss, R.; Scatton, B.; Maffrand, J. P.; Le Fur, G. *J. Pharmacol. Exp. Ther.* **2002**, *300*, 1122.
6. Serradeil-Le Gal, C.; Raufaste, D.; Derick, S.; Blankenstein, J.; Allen, J.; Pouzet, B.; Pascal, M.; Wagnon, J.; Ventura, M. A. *Am. J. Physiol. Regul. Integr. Comp. Physiol.* **2007**, *293*, R938.
7. Serradeil-Le Gal, C.; Wagnon, J.; Tonnerre, B.; Roux, R.; Garcia, G.; Griebel, G.; Aulombard, A. *CNS Drug Rev.* **2005**, *11*, 53.
8. Takano, A. *Nihon Shinkei Seishin Yakurigaku Zasshi* **2009**, *29*, 61.
9. Lubisch, W. U.S. Patent 0,185,126 A1, 1995.
10. (a) Shintani, R.; Inoue, M.; Hayashi, T. *Angew. Chem., Int. Ed.* **2006**, *45*, 3353; (b) Lai, H.; Huang, Z.; Wu, Q.; Qin, Y. *J. Org. Chem.* **2008**, *74*, 283.
11. Pike, V. W. *Trends Pharmacol. Sci.* **2009**, *30*, 431.
12. Hernando, F.; Schoots, O.; Lolait, S. J.; Burbach, J. P. *Endocrinology* **2001**, *142*, 1659.